Novel States of Matter at Low and Ultra-Low Temperatures

Manuel Brando[#], Christoph Geibel, Elena Hassinger, Seunghyun Khim, Markus König, Javier F. Landaeta, Andrew P. Mackenzie and Konstantin Semeniuk

In solid crystals, phases of matter are generally very stable against external perturbations. Large pressure or very high magnetic fields are required to change a thermodynamically stable state at a constant temperature. It has been argued that multiple phases, which are quasi-degenerate in energy, can exist in the vicinity of a quantum critical point (QCP), the point at zero temperature that separates two different states of matter. Such a degeneracy allows tuning between these phases by small external perturbations. This concept has led to the discovery of unconventional superconductivity in many different materials, such as heavy-fermion (HF) or iron-based superconductors. We present here two novel states of matter found at low temperatures in the vicinity of QCPs in two HF systems, $YbRh_2Si_2$ and $CeRh_2As_2$. Both compounds were discovered in our institute and are unconventional superconductors. More specifically, we show that $YbRh_2Si_2$ undergoes a unique electro-nuclear phase transition from a weak magnetically ordered state into a modulated magnetic state at a temperature as low as 1.5 mK, whereas $CeRh_2As_2$ may host the first example of a 'quadrupole density wave' below 0.5 K, a theoretically complex ordering pattern among free electrons that has not yet been observed.

Electro-nuclear order in $YbRh_2Si_2$

$YbRh_2Si_2$ is a canonical heavy-fermion (HF) compound which shows weak antiferromagnetic (AFM) order below $T_N = 70$ mK. This very small ordering temperature signalizes that this compound is near a magnetic QCP. The AFM state was thought to be stable down to zero temperature. However, superconductivity was recently discovered at the ultra-low temperature $T_c = 2$ mK [1]. This discovery was unexpected because it is a rare phenomenon in Yb-based HF compounds, β-$YbAlB_4$ ($T_c = 80$ mK) is the only other known superconducting material in this class. Since this transition was observed together with a large jump in the specific heat capacity $C(T)$ seen at a temperature T_A very close to T_c - associated with ordering of the nuclear moments of the two Yb isotopes ^{171}Yb and ^{173}Yb - it was suggested that the suppression of the weak AFM order by nuclear ordering promotes the emergence of superconductivity [1]. But no clear understanding of the nature of the transition at T_A could be provided.

While superconductivity was first demonstrated by AC-susceptibility measurements, high-resolution resistivity and heat capacity measurements were considered extremely difficult to be realized at such ultra-low temperatures. A resistivity measurement was deemed infeasible in as-grown crystals, as resistive dissipation in the contacts is prohibitively high. Also, in heat capacity measurements, the difficulties to know the exact temperature of the bulk sample limited the precision of the measurements. These problems caused very large error bars in both experiments [1, 2].

In order to be able to perform resistivity and heat capacity measurement with outstanding resolution we have employed two new techniques: We decided to pattern

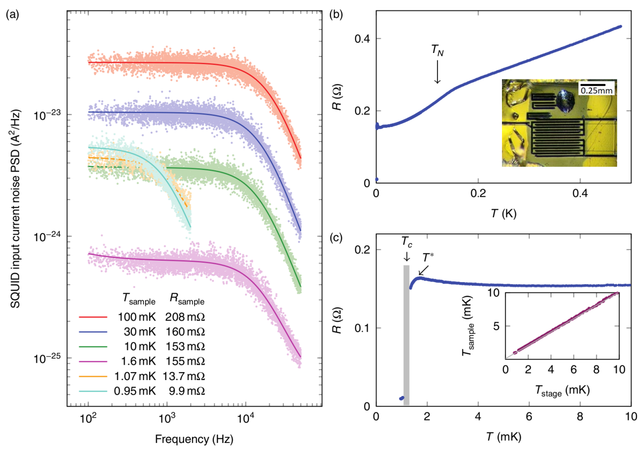

Fig. 1: Noise measurements of the $YbRh_2Si_2$ meander down to ultra-low temperatures at Earth's field: (a) PSD of the current measured by the SQUID current sensor as a function of frequency and fits (cf. [4]). (b) Temperature dependence of the resistance of the meander extracted from noise measurements across the AFM transition at $T_N = 120$ mK. The transition is as sharp as that measured in bulk samples. Inset: Photo of the used meander. (c) Resistance of the meander for temperatures below 10 mK, lowest sample temperature = 0.95 mK. The grey region indicates the temperature range $T_c = 1.2 \pm 0.1$ mK, were strong resistance fluctuations prevent reliable estimation of the sample resistance and temperature. We attribute T_c to the superconducting transition, as the resistance drops by more than an order of magnitude across this narrow temperature range, with an onset at 1.6 mK. The inset shows a linear plot of the sample temperature versus the stage temperature, indicating excellent thermalization of the meander down to 1 mK. Figure taken from [3] ©2022 The Authors, publ. by IOP Publishing.

a bulk sample into a meander geometry by microstructuring using focused-ion-beam (FIB) technique as illustrated in Figure 1b. The resulting amplification of the resistive signal enables a significant increase of signal-to-noise ratios. We could achieve high resolution and ultra-low temperatures by using SQUID-based current-sensing noise thermometry [4], using the sample itself as sensor [3]: The sample temperature $T(K)$ and its resistance $R(\Omega)$ were inferred from fitting the power spectral density (PSD) of the SQUID input current noise, as exemplarily shown in Figure 1a.

The high-resolution resistivity data are plotted in Figure 1b and c. We observe a sharp AFM transition at $T_N = 120$ mK, at higher T than in bulk samples because of strain induced from the substrate to the meander [3]. On cooling below 10 mK we observe a steep decrease with onset at $T^* = 1.6$ mK. Between 1.1 and 1.3 mK (grey area in Figure 1c), strong resistance fluctuations were observed, and the sample resistance and temperature could not be reliably inferred. The resistance drops by more than an order of magnitude over this temperature range, therefore we associate it with the superconducting transition temperature $T_c = 1.2 \pm 0.1$ mK. We observe that T^* is close to the temperature $T_A \approx 2$ mK of the proposed electro-nuclear magnetic transition [1], and suggest that T^* may be the resistive signature of T_A.

To gain more insight into the origin of the transition at T_A we have designed a compact calorimeter for ultra-low temperatures in which the $YbRh_2Si_2$ sample is thermalized via an aluminium wire, operating as a superconducting heat switch. A superconducting solenoid both provides the sample field and operates the heat switch. Heater and noise thermometer, made out of PtW ribbons, are connected to the sample via spot-welded gold wires (more details in Ref. [5]).

The results of such experiment are summarized in Figure 2 which shows the heat capacity data taken with remarkably-high resolution and within a challenging temperature range of 180 μK – 80 mK. The two magnetic phase transitions can be seen at $T_A = 1.5$ mK and $T_N = 70.5$ mK. It can be shown that the heat capacity measured around 1 mK exceeds the heavy-electron term by 3 orders of magnitude and only arises from the nuclear isotopes with natural abundances 0.1431 and 0.1613, respectively, distributed randomly across Yb sites. In Ref. [6] it is demonstrated that the state below $T_A = 1.5$ mK is a new AFM electronic state, with larger ordered moments of the Yb $4f$-electrons. The hyperfine interaction between the tiny nuclear moments and the much larger electron moments favors states with large magnetic polarization of both the electrons and the nuclear moments. At T_A this interaction drives a 'nuclear assisted' transition into a state in which the electronic magnetism appears to be stronger and spatially modulated. This is illustrated in Figure 3 in which the heat capacity of $YbRh_2Si_2$ below T_A is fitted with spatially modulated electronic order (SMO) state (inset of Figure 3), with a sinusoidal distribution of the hyperfine field on the randomly distributed ^{171}Yb and ^{173}Yb nuclei produced by the electronic moments. So, the polarization of the nuclear moments results in a spectacular phase transition between two states which differ in energy only by 1.5 mK. The observation of superconductivity below T_A opens an intriguing possibility that superconductivity and SMO may be intertwined, forming a pair density wave.

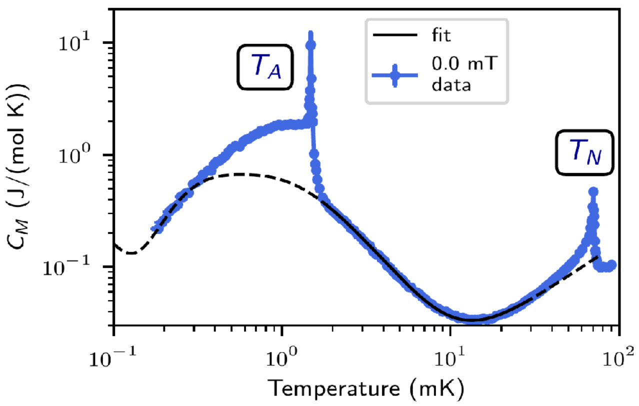

Fig. 2: Molar heat capacity in zero field of the compound $YbRh_2Si_2$. Two sharp anomalies can be seen: While the one at $T_N = 70.5$ mK indicates an electronic transition from a paramagnetic state into an antiferromagnetic state, the anomaly at $T_A = 1.5$ mK reflects a cooperative magnetic transition involving both nuclei and electrons. Note that the lowest point was taken at 180 μK. Figure taken from [6] ©2023 The Authors, publ. by APS.

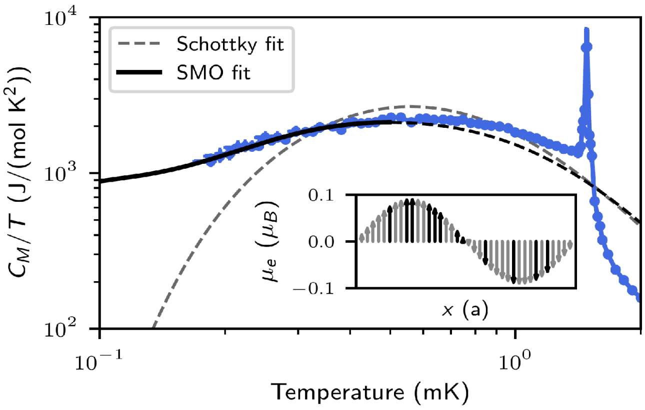

Fig. 3: Zero field C_M/T fitted by the SMO model below 0.5 mK; the "best fit" according to spatially homogeneous Schottky model clearly disagrees with the data. Inset: electronic moments in SMO, black arrows represent randomly distributed Yb sites with active nuclei. Figure taken from [6] ©2023 The Authors, publ. by APS.

Quadrupole density wave order in $CeRh_2As_2$

Free conduction electrons in a periodic environment – such as a crystalline metal – can organize themselves into ordered states with a spatial modulation of their charge or magnetic dipoles. Such ordered states are called charge density waves (CDW) and spin density waves (SDW), respectively. Basic electrodynamics allows for patterns more complex than a point charge or a magnetic dipole, such as electric quadrupoles. However, free electrons do not carry quadrupoles and, accordingly, a quadrupole density wave (QDW) formed by conduction electrons has not been reported yet.

In this respect, the discovery of the unconventional superconductor $CeRh_2As_2$ was crucial [7, 8, 9, 10]. This compound attracted considerable attention from the community because it is the first Ce-based multiphase superconductor characterized by a field-induced transition from an even-parity low-field state (SC1 in Figure 5) to an odd-parity high-field state (SC2) (for more details see **PQM_06_Khim** and Status Report **section 1.10**). Recent improvements in sample quality have resulted in an increase of T_c as well as the sharpness of the phase transition (cf. Figure 4): For instance, the superconducting transition at $T_c = 0.36$ K in a sample of new generation can be seen in the specific heat plotted in Figure 4 and compared to that of a old-generation sample.

In this report, however, we focus on the second transition visible at $T_0 = 0.54$ K. In the first generation of samples (red points in Figure 4) this transition was so weak that doubts were raised about its existence, but in the new generation of samples it becomes as sharp as the superconducting transition.

In the last years we have performed a comprehensive study of several thermodynamic, transport and magnetic properties of the phase below T_0, labeled 'phase I' in Figure 5. All findings point to the presence of a rare case of a non-magnetic, possibly multipolar phase: The absence of an anomaly in magnetic probes, the increase of the transition temperature with magnetic field $H_\perp$ perpendicular to the crystallographic c-axis and with pressure [11]. Also the anisotropy of the magnetic phase diagrams indicated the presence of multipolar degrees of freedom in phase I [11, 12]. This is shown in Figure 5 and Figure 6: For $H \parallel c$ (Figure 5), T_0 monotonically decreases with increasing field and the phase I boundary line enters the superconducting odd-parity phase SC2, suggesting that phase I still exists within the SC2 state. On the other hand, T_0 is almost constant for $H \perp c$ (Figure 6) up to 5 T and then increases steeply. At a critical field $H_{cr} \sim 9$ T a 1^{st}-order phase transition into another phase (phase II) is detected.

While all experimental observations pointed to the presence of multipolar degrees of freedom in the groundstate, the tetragonal crystalline electric field (CEF) level scheme of the localized $4f$-electrons of Ce^{3+} seems to prohibit such order. As illustrated in Figure 7, the $J = 5/2$ multiplet is split by the CEF into three Kramers

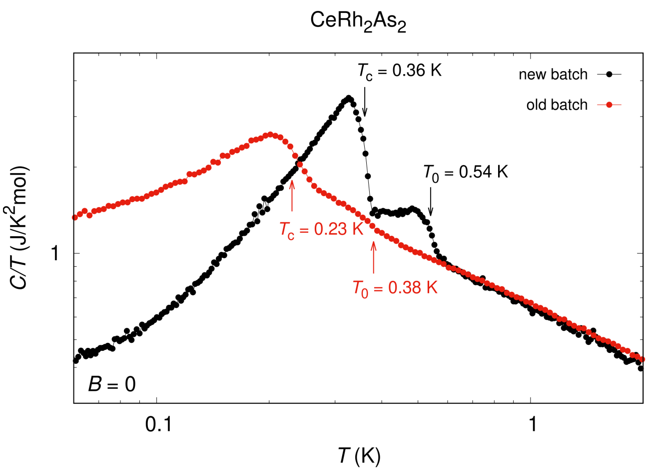

Fig. 4: Temperature dependent specific heat measured in an old-generation sample published in Ref. [7] compared to that of a new-generation sample published in Ref. [15]. Figure taken from [15].

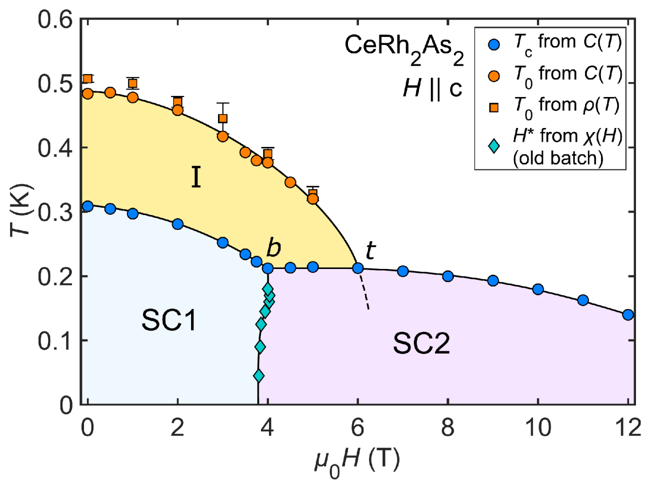

Fig. 5: Temperature-c-axis magnetic field ($T-H$) phase diagram of $CeRh_2As_2$ depicting the two superconducting (SC) states SC1 and SC2 and the ordered phase I. Critical temperatures for the SC states and phase I (T_c and T_0, respectively) were determined by measurements of specific heat $C(T)$ and electrical resistivity $\rho(T)$ conducted on new-generation samples. The SC1-SC2 phase boundary, terminating in a bicritical point b, is plotted according to earlier ac magnetic susceptibility $\chi(H)$ data [7]. The solid black lines are guides for the eye. The dashed line marks a segment of a so far undetected hypothetical phase boundary expected from thermodynamic considerations, while t marks the corresponding tetracritical point. Figure taken from [12] ©2023 The Authors, publ. by APS.

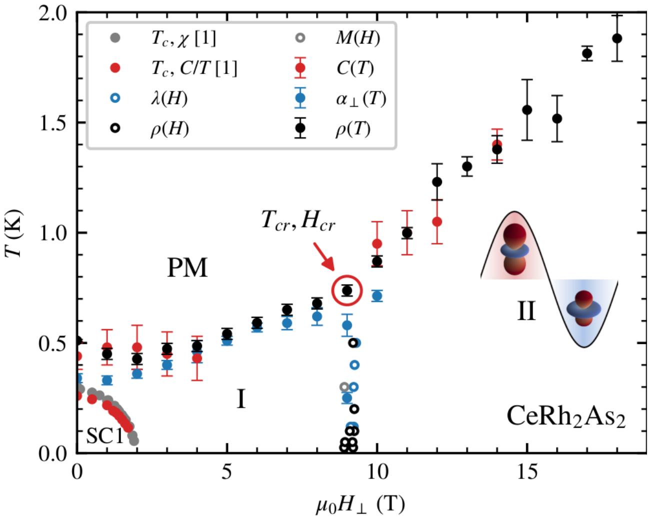

Fig. 6: Magnetic phase diagram of $CeRh_2As_2$ determined by several thermodynamic and transport probes listed in the inset: χ is the magnetic susceptibility, C the specific heat, λ the magnetostriction, ρ the electrical resistivity, M the magnetization and α the thermal expansion. SC1 indicates the even-parity superconducting phase. At a critical field of about 9 T phase I changes into phase II. The inset is a simplistic illustration of a possible QDW. Figure taken from [11] ©2022 The Authors, publ. by APS.

doublets. The groundstate doublet $\Gamma_7^{(1)}$ is separated from the first excited state by about $\Delta \approx 30$ K. Thus, at $T_0 = 0.5$ K only the CEF ground state is populated, which does not bear quadrupolar degrees of freedoms, and therefore, quadrupolar or multipolar order should not be possible.

The material, however, offers one intriguing possibility: Its Kondo temperature $T_K \approx 30$ K is of the same magnitude as Δ [7]. We could demonstrate in Ref. [11] by renormalized-band-structure calculations that T_K affects substantially the quadrupole moment of the CEF-split $4f$ states in $CeRh_2As_2$ because $T_K \approx \Delta$. This is schematically illustrated in Figure 7: The formation of the heavy-Fermi-liquid state leads to a significant admixture of excited CEF states into the low-energy states, because of broadening of the CEF levels (red lines in Figure 7) due to the Kondo effect. This allows the presence of quadrupolar degrees of freedom in the groundstate Kramers doublet and can induce a 'quadrupole density wave' (QDW) by nesting of part of the relevant Fermi surface sheets [11]. This also implies the presence of a quadrupolar QCP and strong quadrupolar fluctuations above this phase.

Quadrupolar ordering at such low temperature is extremely demanding to prove. Techniques like resonant inelastic X-ray scattering (RIXS), for instance, are limited to temperatures above 2 K. Therefore, there is currently no direct evidence of this QDW state.

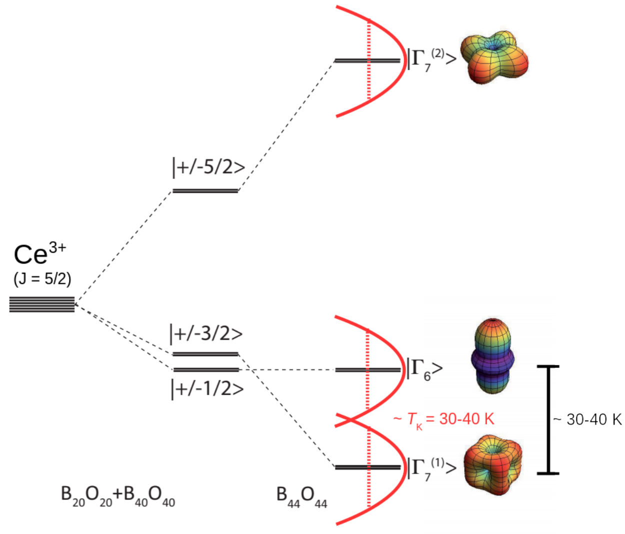

Fig. 7: Proposed CEF scheme for $CeRh_2As_2$: Different contributions $B_{lm}O_{lm}$ of the CEF split the Ce^{3+} $J = 5/2$ multiplet into three Kramers doublets. The broadening of the energy levels due to the Kondo hybridization is schematically illustrated by red lines. Figure taken from Ref. [11] ©2022 The Authors, publ. by APS.

Recent nuclear quadrupole resonance (NQR) and nuclear magnetic resonance (NMR) experiments [10, 13, 14] as well as muon spin resonance (μSR) experiments [15] on new generation of samples have provided clear evidence of dipolar order below T_0, thus questioning the presence of a QDW in phase I. An elegant and reliable solution has been proposed by the authors of Ref. [16] who could reproduce both magnetic phase diagrams (for H parallel and perpendicular to the c-axis) as well as the phase transition at H_{cr}. In their model, the primary order in phase I is AFM (dipolar) with in-plane moments that induce a quadrupole order (phase II) of the O_{xy} type with in-plane field. Therefore, if not in phase I, the QDW should at least exist in phase II.

External Cooperation Partners

K. Ishida, S. Kigatawa, Y. Yanase (University of Kyoto, Japan); A. Rost, P. Wahl (St. Andrews, UK); J. Wosnitza, F. Bärtl, T. Kotte, S. Hamann (HZDR Rossendorf, Germany); D. Agterberg (Wisconsin, USA); P. Brydon (University of Otago, New Zealand.); E.-O. Eljaouhari, G. Zwicknagl (TU Braunschweig, Germany); S. Mishra, I. Sheikin (LNCMI-EMFL, Genoble, France); A. Steppke (University of Zurich, Swissland); K. Kliemt, C. Krellner, M. Kopp, M. Lonsky, J. Müller (Goethe University, Frankfurt, Germany); J. Knapp, L. V. Levitin, J. Nyéki, A. F. Ho, B. Cowan, J. Saunders (RHUL London, UK).

References

[1] *Emergence of superconductivity in the canonical heavy–electron metal $YbRh_2Si_2$*, E. Schuberth, M. Tippmann, L. Steinke, S. Lausberg, A. Steppke, M. Brando, C. Krellner, C. Geibel, R. Yu, Q. Si, and F. Steglich, Science **351** (2016) 485, https://www.science.org/doi/10.1126/science.aaa9733

[2] *Superconductivity in an extreme strange metal*, D. H. Nguyen, A. Sidorenko, M. Taupin, G. Knebel, G. Lapertot, E. Schuberth, and S. Paschen, Nat. Comm. **12** (2021) 4341, https://doi.org/10.1038/s41467-021-24670-z

[3]* *Microstructuring $YbRh_2Si_2$ for resistance and noise measurements down to ultra-low temperatures*, A. Steppke, S. Hamann, M. König, A. Mackenzie, K. Kliemt, C. Krellner, M. Kopp, M. Lonsky, J. Müller, L. V. Levitin, J. Saunders, and M. Brando, New J. Phys. **24** (2022) 123033, https://dx.doi.org/10.1088/1367-2630/aca8c6

[4] *Current Sensing Noise Thermometry: A Fast Practical Solution to Low Temperature Measurement*, A. Casey, F. Arnold, L. V. Levitin, C. P. Lusher, J. Nyéki, J. Saunders, A. Shibahara, H. van der Vliet, B. Yager, D. Drung, Th. Schurig, G. Batey, M. N. Cuthbert, and A. J. Matthews, New J. Phys. **175** (2014) 764, https://link.springer.com/article/10.1007/s10909-014-1147-z

[5]* *Precise Calorimetry of Small Metal Samples Using Noise Thermometry*, J. Knapp, L. V. Levitin, J. Nyéki, M. Brando, J. Saunders, submitted. arXiv:2407.01434 https://arxiv.org/abs/2407.01434

[6]* *Electronuclear Transition into a Spatially Modulated Magnetic State in $YbRh_2Si_2$*, J. Knapp, L. V. Levitin, J. Nyéki, A. F. Ho, B. Cowan, J. Saunders, M. Brando, C. Geibel, K. Kliemt, and C. Krellner, Phys. Rev. Lett. **130** (2023) 126802, https://journals.aps.org/prl/abstract/10.1103/PhysRevLett.130.126802

[7]* *Field-induced transition within the superconducting state of $CeRh_2As_2$*, S. Khim, J. F. Landaeta, J. Banda, N. Bannor, M. Brando, P. M. R. Brydon, D. Hafner, R. Küchler, R. Cardoso-Gil, U. Stockert, A. P. Mackenzie, D. F. Agterberg, C. Geibel, and E. Hassinger, Science **373** (2021) 1012, https://www.science.org/doi/10.1126/science.abe7518

[8]* *Field-Angle Dependence Reveals Odd-Parity Superconductivity in $CeRh_2As_2$*, J. F. Landaeta, P. Khanenko, D.C. Cavanagh, C. Geibel, S. Khim, S. Mishra, I. Sheikin, P.M.R. Brydon, D.F. Agterberg, M. Brando, and E. Hassinger, Phys. Rev. X **12** (2022) 031001, https://doi.org/10.1103/PhysRevX.12.031001

[9]* *Conventional type-II superconductivity in locally noncentrosymmetric $LaRh_2As_2$*, J. F. Landaeta, A. M. Leon, S. Zwickel, T. Lühmann, M. Brando, C. Geibel, E.-O. Eljaouhari, H. Rosner, G. Zwicknagl, E. Hassinger, and S. Khim, Phys. Rev. B **106** (2022) 014506, https://doi.org/10.1103/PhysRevB.106.014506

[10]* *Parity Transition of Spin-Singlet Superconductivity Using Sublattice Degrees of Freedom*, S. Ogata, S. Kitagawa, K. Kinjo, K. Ishida, M. Brando, E. Hassinger, C. Geibel, and S. Khim, Phys. Rev. Lett. **130** (2023) 166001, https://dx.doi.org/10.1103/PhysRevResearch.2.013183

[11]* *Possible Quadrupole Density Wave in the Superconducting Kondo Lattice $CeRh_2As_2$*, D. Hafner, P. Khanenko, E.-O. Eljaouhari, R. Küchler, J. Banda, N. Bannor, T. Lühmann, J. F. Landaeta, S. Mishra, I. Sheikin, E. Hassinger, S. Khim, C. Geibel, G. Zwicknagl, and M. Brando, Phys. Rev. X **12** (2022) 011023, https://doi.org/10.1103/PhysRevX.12.011023

[12]* *Decoupling multiphase superconductivity from normal state ordering in $CeRh_2As_2$*, K. Semeniuk, D. Hafner, P. Khanenko, T. Lühmann, J. Banda, J. F. Landaeta, C. Geibel, S. Khim, E. Hassinger, and M. Brando, Phys. Rev. B **107** (2023) L220504, https://doi.org/10.1103/PhysRevB.107.L220504

[13]* *Observation of Antiferromagnetic Order as Odd-Parity Multipoles inside the Superconducting Phase in $CeRh_2As_2$*, M. Kibune, S. Kitagawa, K. Kinjo, S. Ogata, M. Manago, T. Taniguchi, K. Ishida, M. Brando, E. Hassinger, H. Rosner, C. Geibel, and S. Khim, Phys. Rev. Lett **128** (2022) 057002, https://doi.org/10.1103/PhysRevLett.128.057002

[14]* *Two-Dimensional XY-Type Magnetic Properties of Locally Noncentrosymmetric Superconductor $CeRh_2As_2$*, S. Kitagawa, M. Kibune, K. Kinjo, M. Manago, T. Taniguchi, K. Ishida, M. Brando, E. Hassinger, C. Geibel, and S. Khim, J. Phys. Soc. Jpn **91** (2022) 043702, https://doi.org/10.7566/JPSJ.91.043702

[15]* *Coexistence of local magnetism and superconductivity in the heavy-fermion $CeRh_2As_2$ revealed by μSR studies*, S. Khim, O. Stockert, M. Brando, C. Geibel, C. Baines, T. J. Hicken, H. Luetkens, D. Das, T. Shiroka, Z. Guguchia, and R. Scheuermann, submitted. arXiv:2406.16575 https://arxiv.org/abs/2406.16575

[16] *Anisotropic magnetic and quadrupolar $H-T$ phase diagram of $CeRh_2As_2$*, B. Schmidt, and P. Thalmeier, submitted. arXiv:2404.10510 https://arxiv.org/abs/2404.10510

#manuel.brando@cpfs.mpg.de